Hindawi
Journal of Nanomaterials
Volume 2022, Article ID 7740768, 11 pages
https://doi.org/10.1155/2022/7740768

Research Article

Attenuation of Liver Injury via Bicyclol–Bovine Serum Albumin Nanopreparation using a Green Synthetic Approach

Yanchao Liu,[1] **Mengqi Jia**,[1] **An Gao**,[1] **Xucong Huang**,[1] **Xiaojing Li**,[1] **Lingyi Guo**,[2] **Zhenghua Wu**,[1] **Yuan Yu**,[2] **and Guorong Fan**[1]

[1]*Department of Clinical Pharmacy, Shanghai General Hospital, Shanghai Jiaotong University School of Medicine, Shanghai 200080, China*
[2]*Department of Pharmaceutical Science, Faculty of Pharmacy, Naval Medical University, Shanghai 200433, China*

Correspondence should be addressed to Zhenghua Wu; wuzhenghua526@163.com, Yuan Yu; pharmyuu@163.com and Guorong Fan; guorfan@163.com

Received 5 July 2022; Revised 24 September 2022; Accepted 18 October 2022; Published 9 December 2022

Academic Editor: Kondareddy Cherukula

Copyright © 2022 Yanchao Liu et al. This is an open access article distributed under the Creative Commons Attribution License, which permits unrestricted use, distribution, and reproduction in any medium, provided the original work is properly cited.

Bicyclol (BIC) is a traditional antihepatitis drug that is used to treat chronic hepatitis B infections by improving liver function and reducing transaminase levels. Because the extensive use of BIC for treating liver injury is limited by its poor bioavailability, the course of treatment with oral BIC lasted for >6 months. This study aimed to develop a nano-BIC injection to improve its bioavailability and anti-hepatitis efficacy. We used a green synthetic approach to prepare BIC-bovine serum albumin (BSA) nanoparticles (BIC-NPs). Moderate protein denaturation is required to release free thiol groups in the intramolecular reactions of BSA, which may form an intermolecular disulfide network to stabilize the BIC–BSA nanoassembly. Our results showed that the administration of BIC-NPs in rats resulted in a 2.42-fold increase in drug concentration in plasma. Further, nano-BIC injection showed high bioavailability and rapidly achieved therapeutic concentrations. BIC can restore mitochondrial function by scavenging reactive oxygen species. Moreover, we observed that 70 nm NPs can accumulate in the liver, and the nano-BIC injection protected mice from methotrexate-induced liver injury. This study provides an improved strategy for developing a liver-protecting agent to meet various clinical needs of patients.

1. Introduction

Natural products derived from local and traditional medicinal plants are regarded as excellent sources of prototype drugs for treating a wide range of diseases [1, 2]. North *Schisandra chinensis* (Wuweizi) is an effective herb that is used to treat liver diseases [3, 4]. Among several extracted lignans with therapeutic potential based on lignan schizandrin C, bicyclol [5] (BIC, 4,4-dimethoxy-5,6,5′,6-bis(dimethylene-dioxy)-2-hydroxymethyl-2′-methoxy carbonyl biphenyl) is a safe synthetic drug that was approved as a hepatoprotectant by the Chinese Food and Drug Administration in 2004 [6, 7].

BIC possesses numerous bioactive properties, including antioxidative [8], antiviral [9], general anti-inflammatory, and immunoregulatory effects [10]; most importantly, it exhibits pharmacological activity that focuses on the critical activities occurring in the pathogenic stages from liver dysfunction to hepatocarcinogenesis [11]. These findings suggest that BIC possesses powerful chemopreventive properties. Studies have reported that BIC reduces reactive oxygen species levels by restoring mitochondrial function and alleviates liver injury in mice [12, 13]. Although clinical studies regarding liver diseases have reported the therapeutic potential of BIC [14], the oral bioavailability of BIC is extremely low (9% in rats), which may be attributed to the coeffect of P-glycoprotein-mediated efflux and metabolism by CYP3A in the intestine, thus limiting the extrapolation of BIC for therapeutic uses [15]. The pharmacokinetic properties of BIC have a direct influence on biological responses [16, 17]. When administered orally, the increased metabolism of BIC by the hepatic enzymes of the cytochrome P450 family [18] and uridine diphosphate-glucuronosyltransferase (UGT) results in a short half-life [19], and the formation of demethylation and glucuronidation metabolites indicates species and interindividual variability in plasma and tissue exposure [20].

Table 1: Detection of ion pairs and characteristic parameters of mass spectrometry.

Compound	Parention (m/z)	Daughterion (m/z)	Cone (V)	CE (eV)
Bicyclol (BIC)	373	341	20	13
Biphenyl dimethyl dicarboxylate (DDB)	419	387	7	7

Antihepatitis drugs are often ineffective in these patients owing to their low oral bioavailability, and the course of treatment with BIC is >6 months. Nanoencapsulation is an important strategy for improving the pharmacokinetics of drugs and chemicals and targeting specific parts of the body [21, 22]. In particular, it is necessary to focus on parameters such as diameter and surface charge of nanoparticles (NPs) to ensure reduced opsonization and optimal circulation time in plasma [23, 24].

Despite the therapeutic potential of BIC and advantages of its nanoencapsulation, no injectable formulation of BIC-associated NPs has demonstrated adequate bioavailability, good physicochemical profile, or excellent therapeutic effect. Protein polymers, such as bovine serum albumin (BSA), have been extensively used as nanocarriers for the delivery of several drugs and could be used to improve the pharmacokinetics of BIC. The abundance of BSA-binding sites aids in the transport of structurally diverse molecules [25].

A microemulsion system was prepared to improve BIC formulation in vitro. We assembled molecular BSA into larger sized nanostructures, and free thiol groups were released in the intramolecular reactions of BSA via moderate protein denaturation; these free thiol groups were readily accessible for intermolecular cross-linking. Thus, a novel strategy was developed using these nanostructures with reconstructed intermolecular disulfide bond and hydrophobic interaction for efficient BIC loading. This strategy is simple and involves only a few steps, allowing precise control over particle size and homogeneity. The current approach has the advantage of preventing toxic linkers such as glutaraldehyde as well as the chemical modification of the BIC structure. So far, the use of albumin NP formulations for improving the bioavailability of BIC has not been reported. Thus, the new albumin NP delivery system may enhance antihepatitis activity by modifying BIC bioavailability.

2. Material and Methods

2.1. Chemicals. BIC standard (purity >98%) was provided by Beijing Union Pharmaceutical Factory, and Dalian Meilun Biotech Co., Ltd. provided dimethyl dicarboxylate biphenyl (DDB; purity >98%). Further, methotrexate (MTX), sodium dodecyl sulfate (SDS), dithiothreitol (DTT), and urea were purchased from Aladdin Chemistry Co. Ltd. BSA was purchased from Sigma-Aldrich; NaOH and Na_2CO_3 from Sinopharm Chemistry Reagent Co., Ltd; Cell Counting Kit-8 (CCK-8) from Beyotime Institute of Biotechnology; live/dead cell staining assay kit from Thermo Fisher Scientific; fluorescein isothiocyanate (FITC), 4,6-diamidino-2-phenylindole (DAPI) staining solution from Sigma-Aldrich; Dulbecco's modified Eagle's medium (DMEM), fetal bovine serum (FBS) and phosphate-buffered saline (PBS) from HyClone; and serum aspartate aminotransferase (AST) and alanine aminotransferase (ALT) available kits from Jiancheng Bioengineering Institute.

2.2. Development of the Analytical Method. BIC levels were determined using a UPLC–QQQ–MS/MS system equipped with an electrospray ionization (ESI) source (operating in positive mode; Waters Corp., USA). The analysis was performed on a Zorbax C18 column (2.1 × 100 mm, 1.7 μm). The injection volume was 5 μl. Mobile phase A contained 2 mM ammonium acetate in pure water with 0.1% formic acid (v/v), whereas mobile phase B was acetonitrile. Gradient conditions with a flow rate of 0.3 ml/min were as follows: 0–1 min, 20%–90% B; 1–3 min, 90% B; 3–4 min, 90%–20% B, and 4–5 min, 20% B. During the analysis, all samples were stored at 4°C. Selective ion monitoring signals for $[M + Na]^+$ of BIC (m/z 373) and the internal standard DDB (m/z 419) were obtained. Table 1 lists the detailed optimized mass spectrometry parameters. Using 100 μl of rat plasma, the lower limit of quantification was determined as 0.3 ng/ml.

2.3. Synthesis and Characterization of NPs. A previously reported green synthesis approach [26, 27] was used to synthesize NPs. First, a solution of sodium dodecyl sulfate (2% SDS) and DTT (0.15% DTT) was used to eliminate hydrophobic forces and intramolecular disulfide bonds from BSA. Then, the BSA solution was heated to 90°C for 2 hr to liberate free thiol groups, and BIC (in 1.0 ml of 4-morpholineethanesulfonic acid (MES), 0.1 M, pH 4.8, stirred at 70°C for 3 min) was spiked into the BSA solution and magnetically stirred at 770 rpm. Next, the reaction bottle was immersed in an ice bath. Following the thermal drive, molecular BSA was reformed into large-sized nanostructures via the reconstructed intermolecular disulfide bond and hydrophobic interaction. The abundance of binding sites between BIC and BSA nanostructures allowed for efficient BIC loading and NP formation (Figure 1). The treated BSA was redissolved in MES, and BIC-NPs were prepared by adding different mass ratios of BIC in the reaction solution (BIC : BSA = 1 : 2, 1 : 5, 1 : 7.5, and 1 : 10; w/w). The formulations were analyzed to determine the influence of each parameter on the particle diameter and loading capacity (LC%).

The mean particle size and polydispersity index (PDI) were determined by dynamic light scattering (DLS) (Zetasizer Nano ZS, ZEN3690, Malvern) at 25°C. Based on UPLC–QQQ–MS/MS data, LC% and entrapment efficiency (EE%) were calculated using Equations (1) and (2)

$$\text{EE\%} = \frac{\text{Initial BIC} - \text{Free BIC}}{\text{Initial BIC}} \times 100\% \quad (1)$$

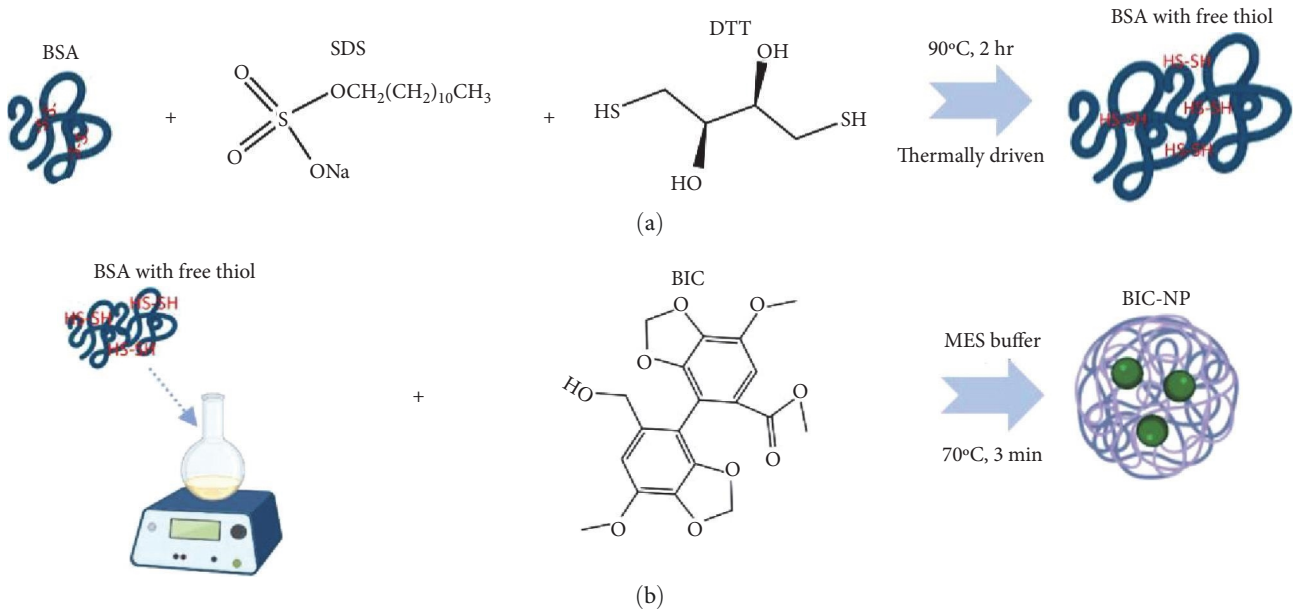

FIGURE 1: Scheme of BIC-NPs preparation: (a) 40 mg/ml BSA, SDS (2%), and DTT (0.15%) solution was used for eliminating hydrophobic forces and intramolecular disulfide bonds, we desaturated BSA using SDS and DTT to liberate free thiols, and then the above BSA solution was heated to 90°C for 2 hr to obtain reduced BSA; (b) the treated BSA was redissolved in MES, while BIC-NPs was prepared by adding BIC into reaction solution.

$$\text{LC}\% = \frac{\text{Weight of BIC in NPs}}{\text{Weight of NPs}} \times 100\%. \quad (2)$$

BIC-NPs were prepared, and the reaction mixture was subjected to ultrafiltration (MWCO: 10,000) with PBS to remove free BIC, excess SDS, and DTT. To obtain the BIC injection, the final suspension was freeze-dried.

2.4. Stability of BIC-NPs. To assess the biostability of BIC-NPs, DLS was used to measure their size changes (0.2 mg/ml) in 5%–10% FBS from 0 to 48 hr at room temperature and different time points. The long-term stability of particles was analyzed from 0 to 90 days. After being treated with a hydrophobic destroyer (1% SDS), disulfide bond destroyer (30 mm DTT), and hydrogen bond destroyer (2 M urea), physical and chemical stabilizing forces for fixing or stabilizing BIC-NPs were determined via DLS. The release behavior of BIC-NPs was evaluated in PBS buffer (pH 7.2 and 5.5) using dialysis bags, and the amount of BIC in releasing medium was measured using the UPLC–QQQ–MS/MS system equipped with an ESI source (operating in positive mode).

2.5. In Vitro Studies Cell Culture. RAW264.7 macrophages and AML-12 mouse hepatocytes cells were obtained from the Cell Resources Center of the Chinese Academy of Sciences and cultured in DMEM supplemented with 10% heat-inactivated FBS and 1% penicillin and streptomycin (v/v). All cells were maintained at 37°C with 5% CO_2 in a constant temperature incubator. Rabbit erythrocytes (5%) were obtained from the Beyotime Institute of Biotechnology.

2.5.1. Safety Evaluation of BIC-NPs. The cytotoxicity of BIC-NPs against AML-12 mouse hepatocytes cells and macrophages (RAW 264.7) was measured spectrophotometrically at 450 nm using Cell Counting Kit-8. These cells were exponentially grown in 96-well cell culture plates (5,000 cells per well) and cultured in DMEM for 24 hr. They were then incubated for 12 hr with different concentrations of BIC-NPs or BIC (equivalent BIC from 1.5 to 100 μg/ml). Cell viability was calculated as a percentage of viable cells as per Equation (3)

$$\text{Viable cells}\% = \frac{\text{Absorbance}_x - \text{Absorbance}_{\text{blank}}}{\text{Absorbance}_0 - \text{Absorbance}_{\text{blank}}} \times 100\%, \quad (3)$$

where Absorbance_0 is the absorbance of untreated cells and $\text{Absorbance}_{\text{blank}}$ is the absorbance of the DMEM medium.

The cytotoxicity of BIC-NPs to macrophages was assayed using a live/dead cell staining assay kit (Thermo Fisher Scientific). Moreover, hemolytic activity was used to assess cytotoxicity to erythrocytes. The 5% rabbit erythrocytes were rinsed thrice with PBS before treatment with the same concentration of BIC-NPs or BIC for 30 min at 37°C. The hemolysis% was measured by measuring the absorbance of the supernatant at 405 nm.

$$\text{Hemolysis}\% = \frac{A_x}{A_w} \times 100\%, \quad (4)$$

A_x is the absorbance of the supernatant of erythrocytes treated with the sample and A_w is the absorbance of the erythrocytes treated with deionized water, which represented 100% hemolysis.

2.5.2. Intracellular Nanoparticle Uptake Analysis. BIC-NPs were stained with FITC, and free FITC was removed by washing three times in PBS and using an ultrafiltration centrifuge tube (10 kD). AML12 mouse cells were incubated with BIC-NPs (FITC-labelled) for 30 min and 4 hr at 37°C and then resuspended at a density of 1.0×10^6/ml with a final concentration of 10 μg/ml DAPI at 37°C for 15 min; finally, the mixture was centrifuged to remove free BIC-NPs.

2.6. In Vivo Experiments Animals. Male Sprague-Dawley (SD, 180–200 g, 6–7 weeks old) rats were obtained from Shanghai Silaike Experimental Animal Co. Ltd. The protocol was approved by the Institutional Animal Care and Use Committee of Shanghai Jiao Tong University (Shanghai, China, approval number: 2021-0008). The rats were housed in an animal room (24 ± 2°C, $60\% \pm 5\%$ relative humidity) under a 12 hr dark/light cycle. Animal studies were conducted following the Guiding Principles for Care and Use of Laboratory Animals. Before the experiment, the rats were given water and fed standard laboratory food for acclimatization for 1 week.

2.6.1. Establishment of Drug-Induced Liver Injury Model. The SD rats in this study were randomly categorized into four groups. The rats in the control group were given 0.9% saline intraperitoneally. For the liver injury groups of high-, medium-, and low-dose MTX, the rats were intraperitoneally injected with 40, 30, and 20 mg/kg MTX, respectively. Blood samples were collected at 6, 12, 18, 24, 36, and 48 hr after injection and then centrifuged at 6,500 rpm and 4°C for 10 min to obtain serum samples, which were transferred to Eppendorf tubes and stored at −80°C for further analysis. The body weights of the rats were recorded daily, and serum AST and ALT levels were determined (as liver function tests) according to the manufacturer's instructions.

2.6.2. Pharmacokinetic Behaviour and Therapeutics of BIC-NPs. Based on the results of the liver injury model, the optimal dose of 30 mg/kg MTX was selected, and the rat liver injury model was established by injecting MTX. The pharmacokinetic behavior and therapeutic potential of BIC and BIC-NPs in the rats after liver injury were investigated. The rats were administered with BIC-NPs or BIC at a dose of 5 mg/kg, and model and blank control groups were set up simultaneously. For oral administration, BIC was suspended in 0.5% aqueous methylcellulose, and BIC-NPs were used for intravenous administration. Blood samples were obtained at 0.083, 0.25, 0.5, 0.75, 1, 2, 3, 6, 9, 12, and 24 hr after injection ($n = 5$). Plasma was harvested via centrifugation at 13,000 rpm for 10 min and stored at −80°C for analysis. Serum samples were collected at 18 and 24 hr after injection, and AST and ALT levels were determined according to the manufacturer's instructions. At 24 hr after liver injury, the rats were sacrificed and the liver was removed. Next, liver tissues were fixed in 10% neutral formalin for hematoxylin–eosin staining. Subsequently, Phoenix WinNonlin 8.1 was used to calculate the pharmacokinetic parameters of BIC after administration.

2.7. Statistical Analysis. Statistical analysis of different groups was conducted by one-way analysis of variance with a 5% significance change ($P < 0.05$, SPSS 17.0, SPSS Inc., USA), as shown in the figures: $^*P < 0.05$;$^{**}P < 0.01$;$^{***}P < 0.001$.

3. Results

3.1. Preparation of BIC-NPs. The bioavailability and efficacy of BIC are limited by its poor water solubility. To improve the solubility and bioavailability, we prepared and characterized BIC-NPs with different BIC proportions (BIC: BSA (weight/weight) = 1 : 2, 1 : 5, 1 : 7.5, and 1 : 10). Figures 2(a) and 2(b) present the size and zeta potential of BIC-NPs with different mass ratios of BIC : BSA. Only a slight change was noted in the size of NPs with different mass ratios, and the lowest potential of BIC-NPs was determined to be −15 mV. Precipitates were obtained with the BIC : BSA mass ratio of 1 : 2, and the other mass ratios could form NPs (Figure 2(c)). To increase LC%, BIC-NPs with the BIC : BSA mass ratio of 1 : 5 was selected, and the EE% and drug LC% of BIC-NPs were determined to be 70% and 12.28%, respectively. TEM analysis confirmed that the as-synthesized NPs were uniform in size, dispersible and spherical in shape (Figure 2(d)). Moreover, the particle size of BIC-NPs was ∼70 nm (Figures 2(a) and 2(e)), with a PDI of 0.08.

3.2. Stability Analysis of BIC-NPs. We determined the stability of BIC-NPs in a simulated physiological environment. The BIC-NPs did not disassemble in 10% FBS during 0–24 hr, as indicated by the negligible variation of NP size (Figure 3(a)). No statistical difference was observed in the size of BIC-NPs in 5%–10% FBS during 0–48 hr, and the stability of BIC-NPs from 0 to 48 hr is shown in Figure S1. The physical and chemical forces for stabilizing NPs are shown in Figure 3(b). SDS incompletely dissociated the NPs; however, BIC-NPs could be completely dissociated via the simultaneous treatment with SDS, DTT, and urea, implying that hydrophobic interaction, disulfide bonds, and hydrogen bonds promote the assembly of NPs and that hydrophobic interaction is the primary binding force. Long-term stability analysis of BIC-NPs revealed that their size distribution slightly changes over 90 days, indicating better storage and transportation of NPs (Figure 3(c) and Figure S3). Due to poor aqueous solubility, BIC generally exhibits low oral bioavailability. Figure 3(d) depicts the coagulation behavior of BIC and BIC-NPs at the same concentration; BIC solution coagulated but no coagulation was observed in BIC-NP solution. The dispersibility of nano-BIC increased from 0.04 to 1 mg/ml. Figure S2 depicts the release behavior of BIC from BIC-NPs in PBS buffer (pH 7.2 and 5.5). The cumulative BIC release ratio increased from 0 to 24 hr and maintained a steady rise in the next 24 hr and eventually returned to normal. The cumulative BIC release ratio increased during the initial 6 hr and 68% BIC was released within 48 hr in PBS buffer (pH 5.5).

3.3. Safety Evaluation of BIC-NPs. To evaluate the uptake behavior of hepatocytes, BIC-NPs labeled with FITC were incubated with cells and then observed under laser confocal microscopy (Figure 4(a)). The merged image indicated that BIC-NPs were phagocytized by hepatocytes over time. To investigate whether BIC-NPs affected the viability of

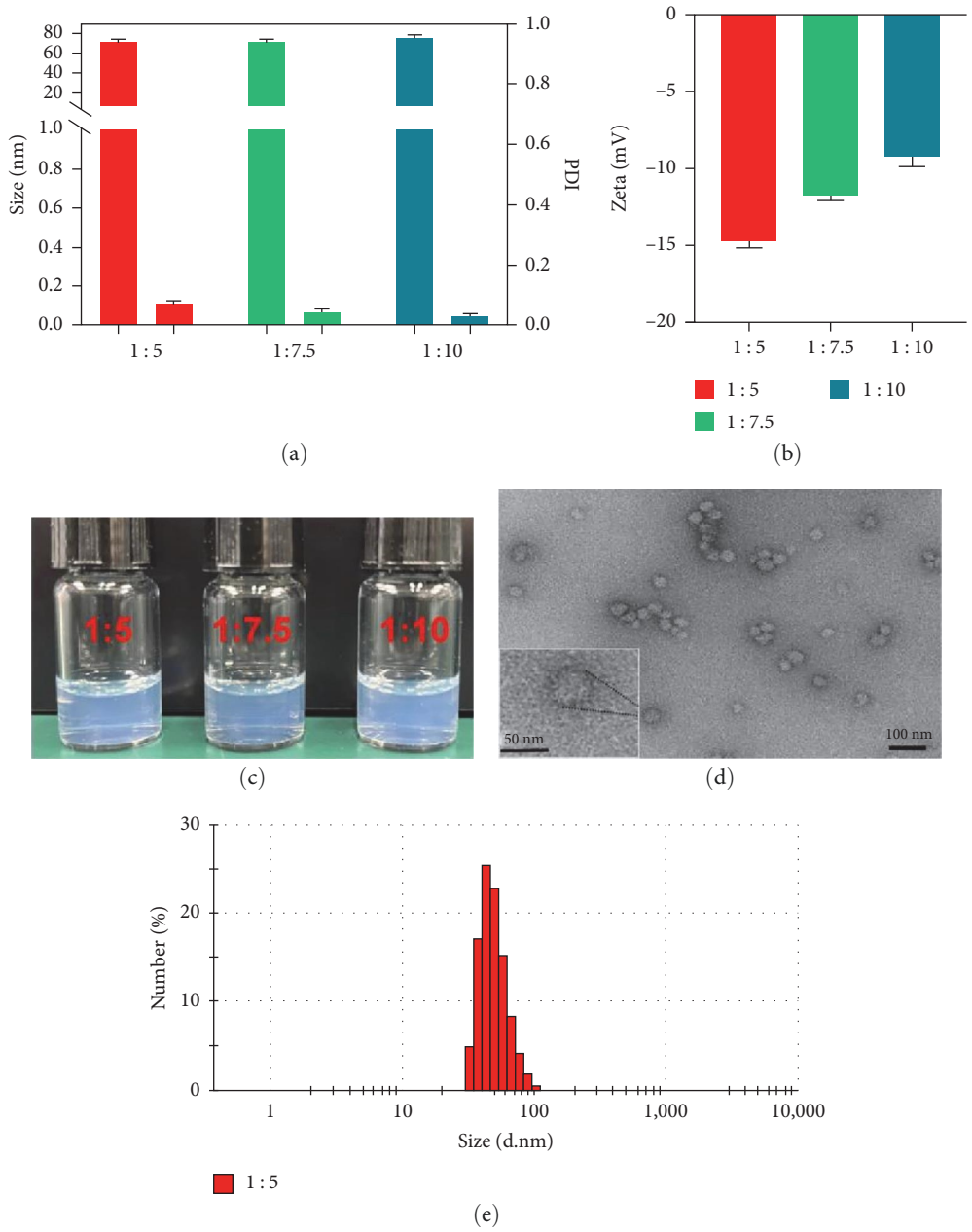

Figure 2: Preparation and characterization of bicyclol nanoparticles (BIC-NPs): (a) size and polydispersity index (PDI) with different BIC-NPs mass ratios; (b) the zeta potential of BIC-NPs is significantly reduced from −9 to −15 mV when BIC/BSA weight ratio is increased from 1 : 10 to 1 : 5 (keep BSA at a constant mass). Data are presented as mean ± SD ($n = 3$); (c) images of BIC-NPs with different mass ratios; (d) transmission emission microscopy (TEM) image of BIC-NPs (BIC : BSA = 1 : 5). Bar = 100 nm; (e) particle size distribution of BIC-NPs with BIC : BSA (w/w) = 1 : 5.

hepatocytes, AML12 mouse cells were incubated with different concentrations of BIC-NPs in vitro (equivalent BIC from 1.56 to 100 μg/ml). No significant cytotoxicity of BIC-NPs was observed (Figure 4(b)). RAW264.7 cells were treated with BIC and BIC-NPs at different concentrations and 37°C for 12 hr, and cell viability was analyzed using a CCK-8 kit to evaluate the cytotoxicity of samples. BIC-NPs showed no obvious toxicity in RAW cells and did not cause obvious apoptosis (cell viability >90%, Figure S4). However, the cells treated with BIC exhibited lower cell viability than those treated with BIC-NPs. The results of staining of the live/dead cells were consistent with those of cell damage (Figure 4(c); green and red fluorescence represent live and dead cells, respectively). Finally, we evaluated the cytotoxicity of BIC-NPs to rabbit cells based on the hemolysis of rabbit red blood cells. BIC-NPs demonstrated no hemolytic effect that was

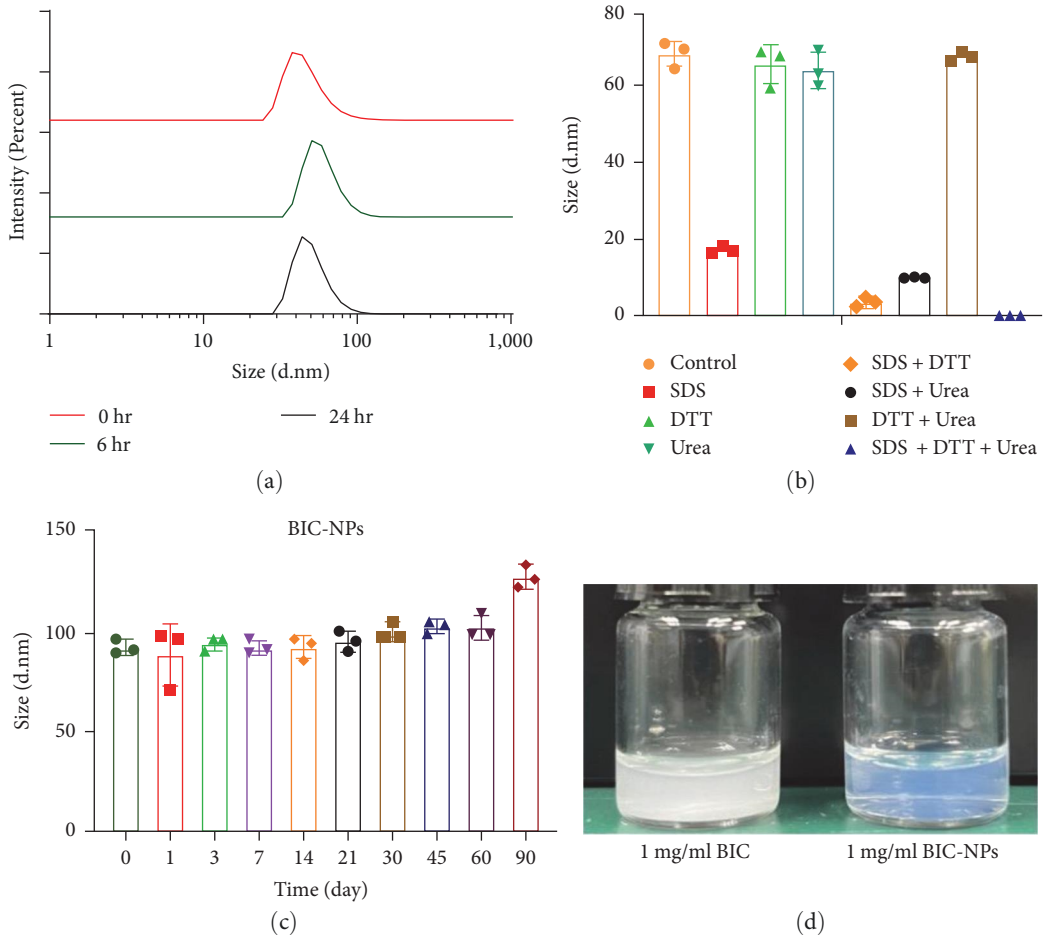

FIGURE 3: Stability analysis of BIC-NPs: (a) stability of BIC-NPs in 10% FBS for 0–24 hr; (b) effect of 1% SDS, 30 mM DTT and 2 M urea on the size of BIC-NPs; (c) long-term stability of BIC-NPs based on a change in size. Data are presented as mean ± SD ($n = 3$); (d) dispersibility of BIC-NPs and BIC with an indicated concentration in PBS buffer (pH = 7.2) at room temperature.

observable with naked eyes on the rabbit red blood cells, even at a concentration of 200 μg/ml (Figures S5(a) and S5(b)).

3.4. Establishment of Liver Injury Model. The biochemical parameters ALT and AST levels are important biomarkers for detecting early liver damage. In this study, AST and ALT levels were analyzed using commercially available kits. Liver injury was initiated via a single intraperitoneal injection of MTX, and AST and ALT levels began to increase after 6 hr. However, compared with the control group, AST and ALT levels were significantly increased in the 40 (Figures 5(a) and 5(b)), 30 (Figures 5(c) and 5(d)), and 20 (Figures 5(e) and 5(f)) mg/kg groups. We hypothesize that the liver injury model based on medium-dose MTX is more universal according to the AST and ALT levels and analysis of behavior in laboratory rats was worse. The decrease in body weight indicates that MTX injections damage the livers of rat; the greatest weight loss was observed in the 40 mg/kg group (Figure S6).

3.5. Pharmacokinetic Data of BIC-NPs and BIC in Rats with Liver Injury. An optimal dose of 30 mg/kg MTX was selected to induce liver injury, we compared the pharmacokinetics within 24 hr of equivalent amounts of BIC and BIC-NPs administered in the liver injury model. Consistent with the improved solubility, the absorption of BIC in NPs prepared using protein (BIC-NPs) was significantly higher than that of BIC suspended in 0.5% Ca−CMC (ratio, 2 : 1; Figure 6(a)). As shown in Table 2, the area under the concentration–time curve (AUC_{0-t}) increased 2.42-fold (1,460.56 vs. 602.83 ng·hr/ml) and the maximum concentration (C_{max}) was increased 9.5-fold (819.02 vs. 86.64 ng/ml) in rats with liver injury. As shown in Supplementary Table S1, $AUC_{0-\infty}$ (h·ng/ml) increased 1.48-fold (1,783.87 vs. 1,198.88 hr·ng/ml). In the liver injury model, the average time to achieve maximum concentration (T_{max}) was 0.35 and 2 hr. Because of improved solubility, extracellular concentrations can rapidly achieve the therapeutic concentration. The apparent total body clearance (CL) was reduced from 3.39 to 2.95 l/hr/kg (BIC vs. BIC-NPs), indicating that the elimination half-life and retention time in vivo were relatively prolonged by BIC-NPs (Table 2).

3.6. The Therapeutics of BIC-NPs in Rats with Liver Injury. The therapeutic effect of BIC on liver injury is limited by its poor oral bioavailability (9% in rats). To further enhance its

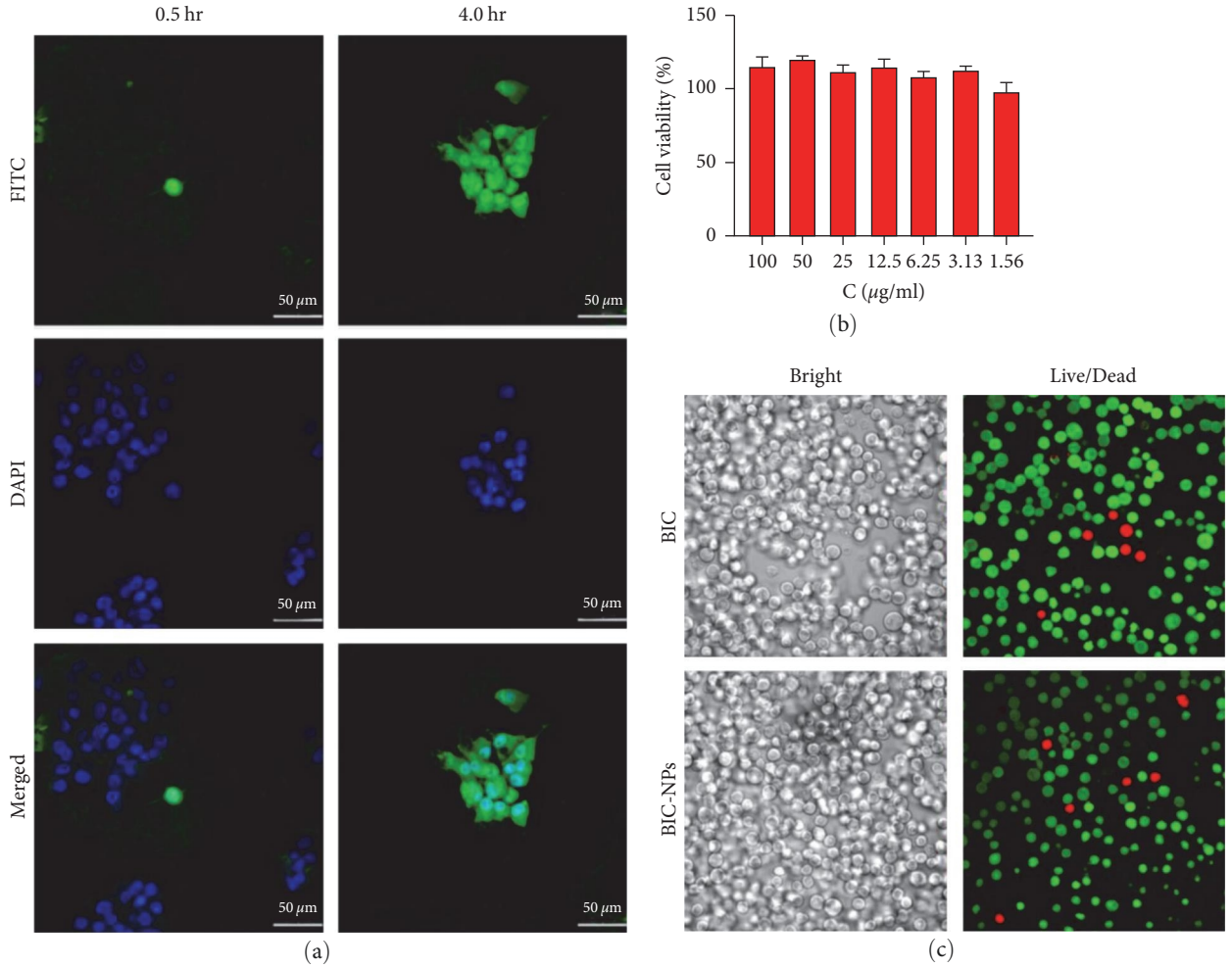

FIGURE 4: Intracellular uptake analysis and safety evaluation of BIC-NPs: (a) the laser scanning confocal images of hepatocyte s incubated with 50 μg/ml BIC-NPs for 30 min, 4 hr at 37°C, hepatocyte, stained with DAPI (blue); BIC-NPs, stained with FITC (green); (b) viability of AML-12 mouse hepatocytes cells in the presence of BIC-NPs from 1.56 to 100 μg/ml for 12 hr. Data are presented as mean ± SD ($n = 4$); (c) live/dead staining of RAW264.7 cells treated with BIC or BIC-NPs (50 μg/ml) for 12 hr. Red and green indicate dead and live cells, respectively.

curative effect, a nano-BIC injection was prepared. According to the pathological results of liver injury in each group, the lobule structure of rat's liver in BIC-NP group was complete, whereas the hepatocytes in the model and BIC groups were damaged and disordered. As shown in Figure 6(b) (red text), hepatic fiber proliferation in the model and BIC groups was thicker than that in the BIC-NPs group, and thicker proliferation usually indicates interstitial liver inflammation.

The pathological changes in rat liver improved via intravenous injection of BIC-NPs. Increased levels of blood AST and ALT are useful for the characterization of enhanced clinical hepatotoxicity. As presented in Figures 6(c) and 6(d), rats were administered with 5 mg/kg BIC-NPs or BIC for treatment following MTX injection. The AST and ALT levels of the BIC-NP group did not increase, whereas those in the model and BIC groups increased at 18–24 hr, with a statistical difference between the BIC and BIC-NP groups at 24 hr ($P < 0.05$). Thus, liver injury showed significant improvement in the BIC-NP group.

4. Discussion

Hepatic dysfunction refers to abnormal liver functioning caused by various factors, such as long-term liver ischemia, drugs, ethanol, infection, and immune processes, which may result in hepatic failure and life-threatening complications. Treatment of hepatic dysfunction remains challenging because of its numerous causes and acute onset. During the treatment of chronic hepatitis B infection, BIC can significantly improve liver function and reduce transaminase levels. Moreover, it exerts an antiviral effect in vitro, with no risk of rebound effect during BIC withdrawal. However, BIC has low solubility in water (0.04 mg/ml), and oral bioavailability in rats can be as low as 9%. The poor bioavailability of BIC is attributed to the P-gp-mediated active efflux and extensive metabolism by CYP3A in the intestines of rats. To address this critical challenge, we developed a "BIC injection" strategy in which low water-soluble drugs are encapsulated into proteins by forming an intermolecular disulfide network.

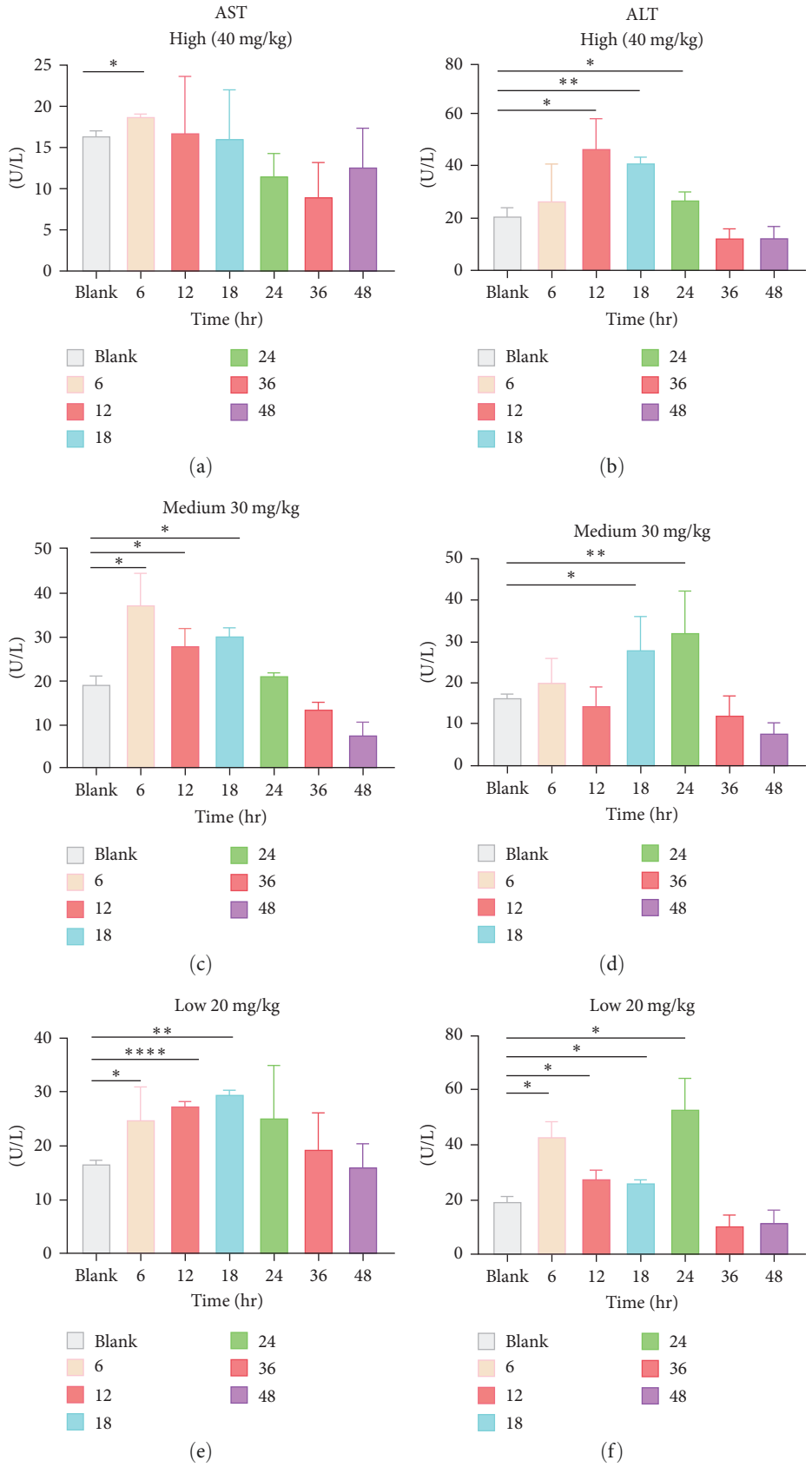

Figure 5: Biochemical indices of liver injury in rats: after intraperitoneal injection of MTX at doses of 40, 30, and 20 mg/kg ($n = 5$), rats blood samples were collected at different time points, and biochemical indices were determined, including (a, c, e) aspartate aminotransferase (AST) and (b, d, f) alanine aminotransferase (ALT). Data are presented as mean ± SD ($n = 5$). $^{*}P < 0.05$, $^{**}P < 0.01$, $^{***}P < 0.001$, and $^{****}P < 0.0001$ vs. blank groups.

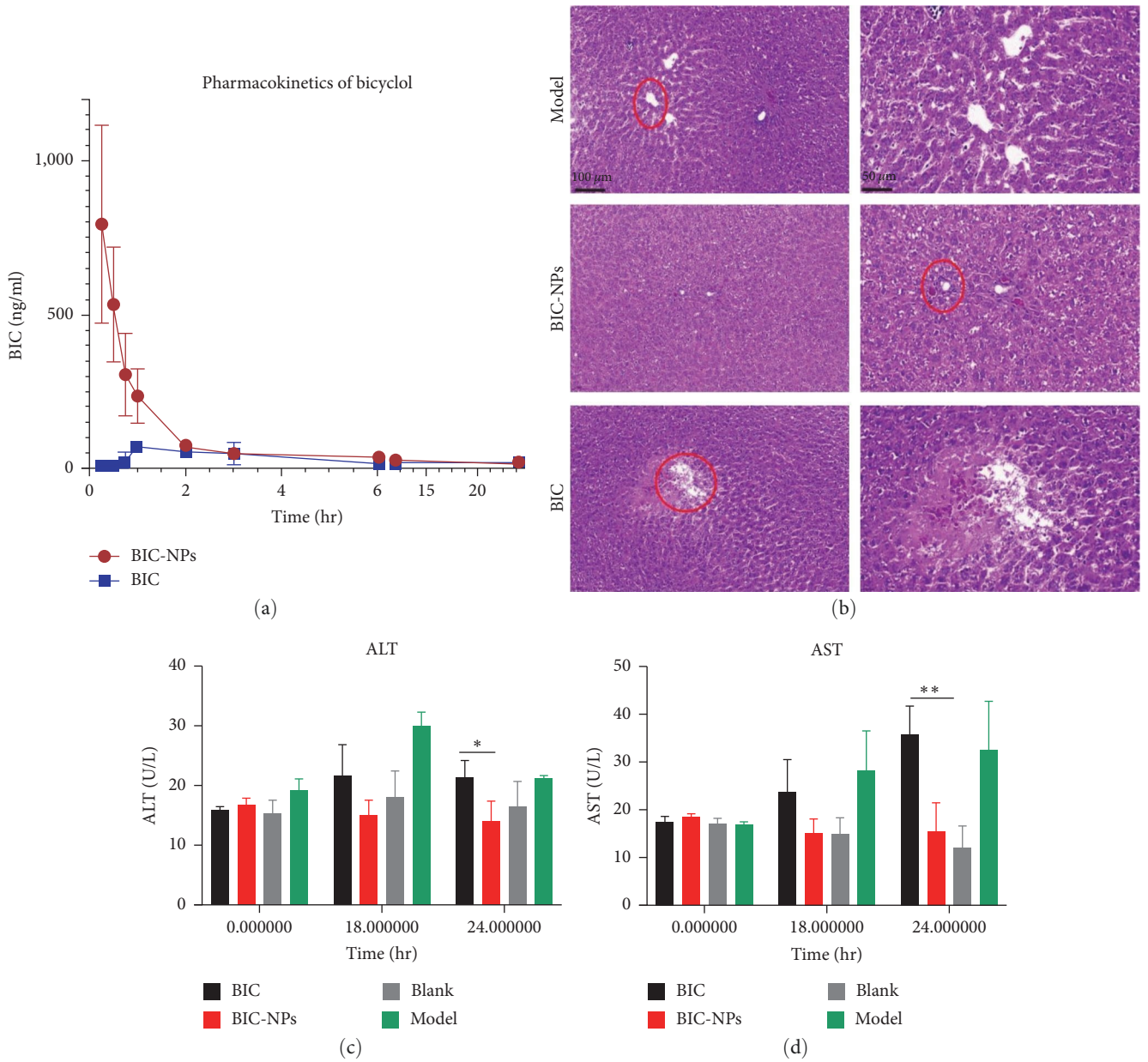

FIGURE 6: Pharmacokinetic behavior and therapeutics of BIC-NPs: (a) plasma concentration–time profiles of BIC in rats after oral administration of BIC suspended in 0.5% CMC or injection of BIC-NPs (dose, 5 mg/kg). Data are expressed as mean ± SD ($n = 5$); (b) representative H&E staining of liver from liver injury rats (for methotrexate) treated with BIC and BIC-NPs; (c and d) ALT and AST levels of liver injury rats. After 24 hr administration of BIC, BIC-NPs to SD rats at a dose of 5 mg/kg, respectively, the normal rats were used as the blank control group (blank). Data are expressed as mean ± SD ($n = 5$). Statistical analysis was performed by one-way factorial ANOVA, $^{*}P < 0.05$, $^{**}P < 0.01$ vs. blank groups.

Albumin is a naturally occurring blood product that is soluble in water and negatively charged in neutral medium. It has the advantages of being safe, nontoxic, nonimmunogenic, degradable, and biocompatible [28]. In 2005, the FDA approved the commercialization of paclitaxel–albumin NP injection developed by the American Life Sciences company. This demonstrates the broad potential of albumin as an intravenous drug carrier [29]. Therefore, research on nanodrug delivery systems using albumin as a carrier has clinical relevance.

For BSA, one free thiol in each BSA molecule cannot ensure sufficient intermolecular cross-linking to form a network at the nanoscale. Moderate protein denaturation is therefore needed to liberate the free thiols and then allowing them to form nanoassembly via intermolecular disulfide networks. In our previous study, NPs were prepared by exposing BSA to liberate free thiols, which were readily accessible for intermolecular cross-linking, NPs were fixed through a disulfide network. The abundance of binding sites between BIC and BSA nanostructures allowed for efficient BIC loading

Table 2: Pharmacokinetic parameters in blood within 24 hr after BIC and BIC-NPs administration of a single dose.

Parameter	BIC	BIC-NPs
T_{max} (hr)	2 ± 1	0.35 ± 0.22
C_{max} (ng/ml)	86.64 ± 13.86	819.02 ± 287.00
CL (l/h/kg)	3.39 ± 1.41	2.95 ± 0.28
$AUC_{0\sim t}$ (hr × ng/ml)	602.83 ± 83.03	$1{,}460.56 \pm 197.06$

T_{max}, C_{max}, CL, and AUC represent the average time to reach maximum concentration, maximum concentration, the apparent total body clearance and the area under the concentration−time curve, respectively.

and NPs formation. The current approach has the advantage of preventing toxic linkers such as glutaraldehyde as well as the chemical modification of BIC structure [27, 30].

We selected BIC-NPs with "maximum drug loading" from different ratios of NPs. The particle size of BIC-NPs was ~70 nm, and PDI was <0.1 (Figure 2). The stabilizing forces in NPs include hydrophobic interaction, disulfide bonds, and hydrogen bonds, which ensure their structural stability in serum. The long-term stability of BIC-NPs was evaluated using basic experiments, and the morphology slightly varied after 90 days (Figure 3). The stability and cytotoxicity of serum should be considered while preparing injection. Thus, the stability of BIC-NPs in a simulated physiological environment was evaluated. The results confirmed that NPs could remain stable in 10% FBS and that the rate of release of NPs was high under acidic conditions (Figures S1 and S2). The results of the intracellular NP uptake analysis revealed that NPs enter hepatocytes and play a role without causing any damage (Figure 4). After incubating BIC-NPs for 12 hr, cytotoxicity experiments confirmed that cell survival was >90% (Figure 4 and Figure S4). The above results indicate that NPs can be used as a carrier for intravenous administration of drugs.

To assess the pharmacokinetics of BIC and BIC-NPs in the liver injury model, a suitable MTX concentration was applied to the liver injury model. Biochemical parameters such as ALT and AST are effective biomarkers for detecting early liver damage. Because the changes in ALT and AST levels were more stable in the medium-dose MTX group, we selected 30 mg/kg MTX to establish the liver injury model (Figure 5). Hepatic dysfunction in patients influences the CL of drugs that are metabolized and excreted by the liver. Thus, it is crucial to reduce the dose of certain drugs in patients with liver diseases. In this study, the solubility of nanomodified BIC increased 25-fold, and the concentration of BIC in blood (P_{blood}) was increased 2.42-fold after the administration of BIC-NPs in the liver injury model (Figure 6(a)). These findings indicate that the pharmacokinetics of BIC-NPs differ significantly compared with that of BIC in SD rats. The enhanced bioavailability may be partly attributed to the increased solubility and distribution of the drug. The BIC-NPs formulation developed in this study demonstrated satisfactory bioavailability and low toxicity; moreover, low-dose protein NPs have an identical therapeutic effect as the original drug for treating liver injuries. Furthermore, our results showed that the new BIC nanoinjection delivery system improved antihepatitis activity by modifying BIC bioavailability. Treatment courses with BIC last for >6 months; therefore, we developed the "BIC injection" with a rapid onset of action, which can exert the therapeutic effect in a shorter time and at a low dose. NPs can enter hepatocytes and restore mitochondrial function; liver injury showed significant improvement in the BIC-NP group (Figure 6). Thus, this study provides an improved strategy for developing a liver-protecting agent to meet various clinical needs of patients.

5. Conclusions

In this study, we used BSA to synthesize BIC-NPs with satisfactory bioavailability, antihepatitis efficacy, and low toxicity via a green synthesis approach. Consistent with the improved in vitro solubility, the bioavailability of BIC-NPs in rats was significantly increased. These results indicate that protein NPs are promising drug delivery systems for improving the bioavailability and therapeutic effect of BIC. Moreover, they provide clinically viable treatment alternatives for patients with liver injuries.

Data Availability

Almost all image and data of samples used to support the findings of this study are included within the article. The data that support the findings of this study are available from the first author.

Conflicts of Interest

The authors declare that they have no conflicts of interest.

Authors' Contributions

Yanchao Liu: investigation, experimental, writing—original draft; Mengqi Jia: writing—review and editing; An-Gao: data processing; Xucong Huang and Xiaojing Li: animal experimental; Lingyi Guo: cell experiment; Zhenghua Wu and Yuan Yu: the main work includes: guiding and perfecting the experimental technology; Guorong Fan: conceptualization, supervision, writing—review and editing.

Funding

This work was financially supported through grants from the National Natural Science Foundation of China (81973289) the Shanghai Sailing Program (21YF1436300).

Supplementary Materials

More information on the physiochemical characterization of nanoparticles, safety evaluation and additional pharmacokinetic characterizations in vivo of BIC-NPs. (*Supplementary Materials*)

References

[1] F. Ntie-Kang, *Drug discovery from African medicinal plants: natural product database development, lead discovery and toxicity assessment; kumulative habilitationsschrift*, Doctoral dissertation, Habilitationsschrift, Halle (Saale), Martin-Luther-Universität, Halle-Wittenberg, 2021.

[2] B. Malleswari and R. Tripura, "New drug development-a review on natural products obtained from medicinal plants as source," *Mukt Shabd Journal*, vol. 9, no. 5, pp. 4977–4982, 2020.

[3] Z. Wu, M. Jia, W. Zhao et al., "Schisandrol A, the main active ingredient of Schisandrae Chinensis Fructus, inhibits pulmonary fibrosis through suppression of the TGF-beta signaling pathway as revealed by UPLC-Q-TOF/MS, network pharmacology and experimental verification," *Journal of Ethnopharmacology*, vol. 289, Article ID 115031, 2022.

[4] Y. Zhou, L. Men, Y. Sun, M. Wei, and X. Fan, "Pharmacodynamic effects and molecular mechanisms of lignans from *Schisandra chinensis* Turcz. (Baill.), a current review," *European Journal of Pharmacology*, vol. 892, Article ID 173796, 2021.

[5] Y. Wang, R. Lai, P. Zong et al., "Bicyclol for the treatment of drug-induced liver injury: a propensity score matching analysis using a nationwide inpatient database," *Journal of International Medical Research*, vol. 49, no. 4, 2021.

[6] T. Zhao, L. Mao, Z. Yu et al., "Therapeutic potential of bicyclol in liver diseases: lessons from a synthetic drug based on herbal derivative in traditional Chinese medicine," *International Immunopharmacology*, vol. 91, Article ID 107308, 2021.

[7] G.-T. Liu, Y. Li, H.-L. Wei et al., "Toxicity of novel anti-hepatitis drug bicyclol: a preclinical study," *World Journal of Gastroenterology*, vol. 11, no. 5, pp. 665–671, 2005.

[8] T.-M. Zhao, Y. Wang, Y. Deng et al., "Bicyclol attenuates acute liver injury by activating autophagy, anti-oxidative and anti-inflammatory capabilities in mice," *Frontiers in Pharmacology*, vol. 11, Article ID 463, 2020.

[9] J. Wu, W. Zheng, L. Rong, Y. Xing, and D. Hu, "Bicyclol exerts an anti-tumor effect via ROS-mediated endoplasmic reticulum stress in human renal cell carcinoma cells," *Biomedicine & Pharmacotherapy*, vol. 91, pp. 1184–1192, 2017.

[10] Y.-W. Zhang, Y.-S. Guo, X.-Q. Bao, H. Sun, and D. Zhang, "Bicyclol promotes toll-like 2 receptor recruiting inosine 5′-monophosphate dehydrogenase II to exert its anti-inflammatory effect," *Journal of Asian Natural Products Research*, vol. 18, no. 5, pp. 475–485, 2016.

[11] H. Sun and G. T. Liu, "Chemopreventive effect of bicyclol on malignant transformation of WB-F344 rat liver epithelial cells and its effect on related signal transduction in vitro," *Cancer Letters*, vol. 236, no. 2, pp. 239–249, 2006.

[12] Y. Wang, "Research progress in mechanism of hepatoprotective and anti-inflammatory by bicyclol," *Chinese Journal of Gastroenterology and Hepatology*, vol. 7, pp. 674–677, 2010.

[13] H. Li, J.-R. Li, M.-H. Huang et al., "Bicyclol attenuates liver inflammation induced by infection of hepatitis C virus via repressing ROS-mediated activation of MAPK/NF-κB signaling pathway," *Frontiers in Pharmacology*, vol. 9, Article ID 1438, 2018.

[14] Y. I. Jianhua, L. I. Wei, and Y. Xiong, "Clinical study on bicyclol against liver fibrosis induced by chronic hepatitis B," *Journal of Clinical Internal Medicine*, vol. 23, no. 1, pp. 57–59, 2006.

[15] W. Tan, H. Chen, J. Hu, and Y. Li, "A study of intestinal absorption of bicyclol in rats: active efflux transport and metabolism as causes of its poor bioavailability," *Journal of Pharmacy & Pharmaceutical Sciences*, vol. 11, no. 3, pp. 97–105, 2008.

[16] B. Wang, Z. Liu, D. Li et al., "Application of physiologically based pharmacokinetic modeling in the prediction of pharmacokinetics of bicyclol controlled-release formulation in human," *European Journal of Pharmaceutical Sciences*, vol. 77, pp. 265–272, 2015.

[17] S. Yang, J. Hu, Y. Li, and Z. Zhao, "Evaluation of pharmacokinetic interactions between bicyclol and co-administered drugs in rat and human liver microsomes in vitro and in rats in vivo," *Xenobiotica*, vol. 49, no. 8, pp. 987–994, 2019.

[18] H. U. Jin-Ping, H. Chen, and L. I. Yan, "Effect of bicyclol on liver microsomal cytochrome P450 isozymes and phase IIenzymes in rats," *Chinese Journal of New Drugs*, vol. 04, pp. 340–348, 2009.

[19] Y.-Y. Ji, N.-N. Cheng, and G.-B. Yao, "Pharmacokinetic study of bicyclol in thirty health volunteers," *Chinese Journal of Clinical Pharmacology and Therapeutics*, vol. 6, no. 3, pp. 218–221, 2001.

[20] M. Hu, Y. Li, F. You et al., "Comparison and identification of metabolic profiling of bicyclol in rats, dogs and humans in vitro and in vivo," *European Journal of Pharmaceutical Sciences*, vol. 154, Article ID 105518, 2020.

[21] H. Rostamabadi, S. R. Falsafi, and S. M. Jafari, "Nanoencapsulation of carotenoids within lipid-based nanocarriers," *Journal of Controlled Release*, vol. 298, pp. 38–67, 2019.

[22] A. Chimento, F. De Amicis, R. Sirianni et al., "Progress to improve oral bioavailability and beneficial effects of resveratrol," *International Journal of Molecular Sciences*, vol. 20, no. 6, Article ID 1381, 2019.

[23] S. Javaid, N. M. Ahmad, A. Mahmood et al., "Cefotaxime loaded polycaprolactone based polymeric nanoparticles with antifouling properties for in-vitro drug release applications," *Polymers*, vol. 13, no. 13, Article ID 2180, 2021.

[24] P. Ghosh, S. Bag, S. Parveen, E. Subramani, K. Chaudhury, and S. Dasgupta, "Nanoencapsulation as a promising platform for the delivery of the Morin-Cu(II) complex: antibacterial and anticancer potential," *ACS Omega*, vol. 7, no. 9, pp. 7931–7944, 2022.

[25] A. O. Elzoghby, W. M. Samy, and N. A. Elgindy, "Albumin-based nanoparticles as potential controlled release drug delivery systems," *Journal of Controlled Release*, vol. 157, no. 2, pp. 168–182, 2012.

[26] K. Wang, S. Wen, L. He et al., ""Minimalist" nanovaccine constituted from near whole antigen for cancer immunotherapy," *ACS Nano*, vol. 12, no. 7, pp. 6398–6409, 2018.

[27] Y. Liu, Y. Han, T. Fang et al., "Turning weakness into strength: albumin nanoparticle-redirected amphotericin B biodistribution for reducing nephrotoxicity and enhancing antifungal activity," *Journal of Controlled Release*, vol. 324, pp. 657–668, 2020.

[28] L. Jiang, Y. Jiang, L. Li et al., "A supramolecular nanocarrier for efficient cancer imaging and therapy by targeting at matriptase," *Journal of Controlled Release*, vol. 334, pp. 153–163, 2021.

[29] M. Gharbavi, H. Danafar, and A. Sharafi, "Microemulsion and bovine serum albumin nanoparticles as a novel hybrid nanocarrier system for efficient multifunctional drug delivery," *Journal of Biomedical Materials Research Part A*, vol. 108, no. 8, pp. 1688–1702, 2020.

[30] Y. Wen, H. Dong, K. Wang, Y. Li, and Y. Li, "Self-Templated, Green-Synthetic, Size-Controlled Protein Nanoassembly as a Robust Nanoplatform for Biomedical Application," *ACS Applied Materials & Interfaces*, vol. 10, no. 14, pp. 11457–11466, 2018.